Poly(ethylene oxide) Single Crystals as Templates for Au Nanoparticle Patterning and Asymmetrical Functionalization

Bing Li,[†] Chaoying Ni,[‡] and Christopher Y. Li*,[†]

A.J. Drexel Nanotechnology Institute and Department of Materials Science and Engineering, Drexel University, Philadelphia, Pennsylvania 19104, and W.M. Keck Electron Microscopy Facility, Department of Materials Science and Engineering, University of Delaware, Newark, Delaware 19716

Received September 10, 2007; Revised Manuscript Received October 29, 2007

ABSTRACT: Considerable attention has been paid to nanoparticle (NP) research because of their fascinating properties and potential applications in nanotechnology and biotechnology. Asymmetrically functionalizing NP is of particular interest because it could directly lead to controlled patterning of NPs for a variety of applications. In this article, we report using 2-dimensional poly(ethylene oxide) (PEO) lamellar single crystals to create a patterned functional (thiol) surface and to immobilize gold NPs (AuNPs). We demonstrate that patterning AuNPs could be achieved by incubating these single crystals with gold sol and the AuNP areal density could be easily controlled by polymer molecular weight as well as the incubation time. Melting and recrystallization of the AuNP-covered PEO single crystals led to dewetting of PEO. AuNP chains were also observed during the recrystallization process, which was attributed to the dendritic growth of edge-on PEO crystals. Furthermore, this unique technique also enables asymmetric functionalization of AuNPs. Free-standing bilayer AuNP/PEO films were obtained. Dissolving PEO single crystals led to free asymmetrically functionalized AuNPs and AuNP complexes. This approach provides a novel means to pattern AuNPs and synthesize asymmetrically functionalized AuNPs. We also anticipate that this methodology could be applied to other metal or semiconductor NPs.

Introduction

Metal and semiconductor nanoparticles (NPs) have attracted considerable attention in recent years due to their fascinating optic and electronic properties and their potential applications in nanotechnology and biotechnology.[1−4] The synthetic methodology has been extensively investigated, and NPs with controlled size and shape can be readily obtained.[1,3,5] The next challenge in the field is achieving ordered NP arrays, which is the critical step to transferring the nanoscale properties to macroscale level for applications such as single electron devices, multifunctional artificial molecules, etc.[1−4,6−9] A number of different methods have been used to fabricate ordered NP structures. Using controlled crystallization of functionalized NPs, ordered NP arrays were obtained.[1−4,10−12] Self-assembly of NPs at the liquid−liquid interface offers another approach. Semiconductor NPs with different sizes were observed to phase separate on a liquid−liquid interface.[13] Block copolymer self-assembly was also used to control the location of NPs.[14−18] It has been realized that size as well as surface chemistry of NPs is critical to the phase behavior of block copolymer/NP systems.[8,19−28]

To prevent agglomeration, NPs are often surface coated with a layer of organic functional molecules. Close packing of these functionalized NPs usually leads to a 2-dimensional (2-D) hexagonal lattice. In order to use assembled NPs for different applications, more complex NP structures, such as chains, sheets, or 3-dimensional pyramids, are often desired. It has been recognized that tailor-made, asymmetrically functionalized NPs (AFNPs) are critical to achieving these complex structures. AFNPs represent a category of NPs with controlled functional groups (both chemistry and particle site specificity) on the particle surfaces (e.g., Janus particles, patchy particles, etc.). While a Janus particle possesses two types of structures on the particle surface, this concept can be extended to "patchy particles" where single or multiple "patches" (functional groups) are attached to the particle surface.[29−31] The well-designed patches or functional groups could directly lead to controlled patterning of NPs into complex structures for a variety of applications.[29−32] Via computer simulation, Glotzer et al. proposed numerous possible assembly routes for patchy particles.[30,31] Chains, sheets, rings, icosahedra, square pyramid, tetrahedral, twisted, and staircase structures were obtained through suitable design of the surface pattern of patches.

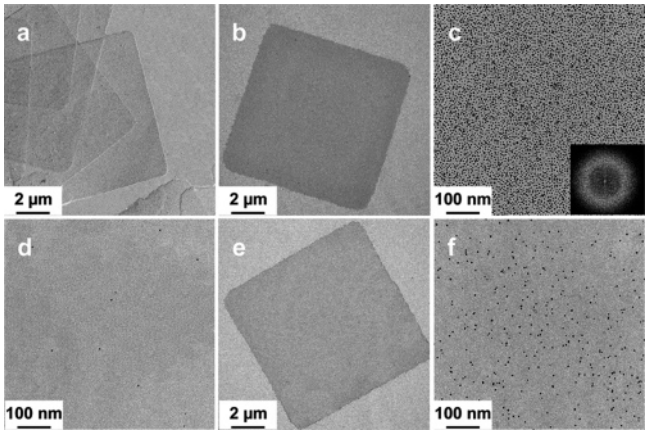

Figure 1. TEM micrographs of (a) HS-PEO(2K) single crystals and (b, c) 5 nm AuNP-covered HS-PEO(2K) single crystals. The inset shows the FFT pattern. (d) HO-PEO(2K) single crystals after incubation with 5 nm AuNPs. (e, f) AuNP-covered HS-PEO(48.5K) single crystals.

Experimentally, on macroscopic scales and under surface tension when dispersed in water, millimeter-sized plastic wedges patterned with patches of solder and hydrophobic lubricant self-assembled to form microelectronic devices whose structure resembles that of the tobacco mosaic virus.[33] In the colloid

* Corresponding author: Ph 215-895-2083; Fax 215-895-6760; e-mail chrisli@drexel.edu.
[†] Drexel University.
[‡] University of Delaware.

10.1021/ma702047k CCC: $40.75
Published on Web 12/06/2007

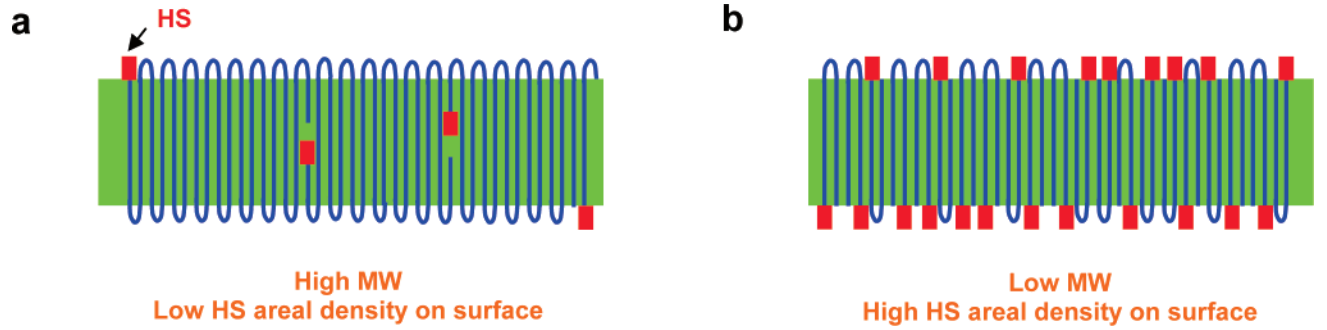

Figure 2. Schematic representations of the cross sections of HS-PEO single crystals (a) nonintegral folding, high molecular weight and (b) integral folding, low molecular weight.

Scheme 1. Experimental Procedure To Fabricate Asymmetrically Functionalized AuNPs

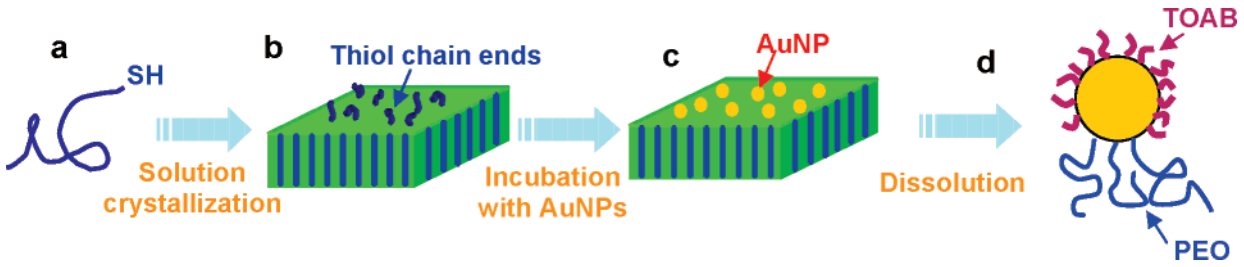

science community, numerous techniques have been developed to synthesize patchy particles with relatively large sizes.[34−37] Whitesites et al. used the thin film deposition technique to coat a thin metal film onto an array of spherical silica colloids, followed by dissolution of the colloidal template. This procedure produced metallic half-shells with nanometer-scale dimensions. Half-shells of gold, platinum, and palladium were fabricated, with diameters of the particles ranging from 100 to 500 nm and shell thickness of 8−15 nm.[38] Electrospray was also used to spin binary polymeric particles (a few hundred nanometers in diameter).[39,40] Despite the extensive efforts dedicated to NP research, it still remains a challenging task to achieve AFNPs with small diameters (<20 nm). A few novel approaches have been reported, most of which either used a kinetic control method or employed a solid-phase substrate to achieve asymmetric NP functionalization. DNA has been used to functionalize NPs.[41−43] Alivisatos et al. used a kinetic control approach to functionalize NPs with as few as one oligonucleotide per particle.[44,45] The resulting AFNPs enabled the assembly of dimer and trimer structures with controlled interparticle distances. Mirkin and co-workers employed a magnetic microparticle [2.8 μm polystyrene (PS) particle with an iron oxide core] as the geometric restriction template and were able to functionalize a AuNP with two different types of oligonucleotides in a site-specific manner.[46] PS Wang resin was also used by a few groups to achieve discrete functionalization on NP surface.[47−51] PS Wang resin particles are a few tens of micrometers in diameter and are often used as the solid substrate in peptide and combinatorial library synthesis.[52] To achieve AFNPs (in this case, a monofunctional group on each AuNP), the functional group (normally −OH) areal density was controlled to be low so that each functional group will only attach to one AuNP. PS Wang resin was functionalized with thiol groups which undergo place exchange reaction with butanethiolate-protected AuNPs. AuNPs with monofunctional groups can thus be achieved.[47,48,50,51] Anisotropic deposition of AuNPs on organic single crystals was also reported.[53]

Our group recently developed a polymer-single-crystal-templating method to synthesize asymmetrically functionalized AuNPs.[54] In this article, we report the detailed study on using poly(ethylene oxide) (PEO) single crystals as the solid-state templates to functionalize selected surface areas of AuNPs. AuNPs were successfully immobilized on thiol-PEO single-crystal surfaces. The areal density of AuNPs was controlled by incubation time as well as the molecular weight of the polymer. The immobilized AuNPs were reorganized into a chain structure upon recrystallization of PEO. Bilayer AuNP/PEO hybrids were also obtained using multiple depositions of AuNPs with different sizes. Subsequent dissolution of the hybrids led to free asymmetric binary AuNP complexes.

Experimental Section

Materials. Thiol-terminated poly(ethylene oxide) (HS-PEO, 2K and 48.5K g/mol) was purchased from Polymer Source Inc. Amyl acetate, hexanedithiol, gold sol (5, 20, and 50 nm), tetraoctylammonium bromide (TOAB), sodium oleate, hexane, magnesium chloride, hydroxyl-terminated poly(ethylene oxide) (HO-PEO, 2K g/mol) and molecular sieves were purchased from Aldrich. All materials were used as received.

Synthesis and Sample Preparation. a. Preparation of HS-PEO Single Crystals Using a Self-Seeding Method. 1.2 mg of HS-PEO(2K) was dissolved in 3.0 g of amyl acetate at 60 °C for 10 min. The solution was quenched to 5 °C for 3 h. The resultant crystal suspension was brought to 41 °C for 10 min to form the crystalline seeds. The solution was then quenched to 24 °C and crystallized for 24 h. The suspension of the single crystals was isothermally filtered at 24 °C to remove the uncrystallized polymers.

For 48.5 K g/mol HS-PEO, the following procedure was applied. 1.0 mg of HS-PEO(48.5K) was dissolved in 10 g of amyl acetate at 60 °C for 10 min. The solution was quenched to 5 °C for 3 h. The resultant crystal suspension was brought to 46 °C for 10 min to form the crystalline seeds. The solution was then crystallized at 38 °C for 2 h. The suspension of the single crystals was isothermally filtered at 38 °C to remove the uncrystallized polymers.

b. Immobilization of 5 nm AuNPs on HS-PEO Single Crystals. The experimental procedure is shown in Scheme 1. 1.0 g of 1.0% TOAB/amyl acetate solution was mixed with 1.0 g of gold sol (5 nm). The mixture was sonicated for 1 min and centrifuged for 10 min at 850*g*. The amyl acetate phase containing AuNPs was collected. A molecular sieve was used to remove the residual water. The HS-PEO single-crystal suspension was drop-cast on a carbon-coated Ni grid or a piece of glass slide, which

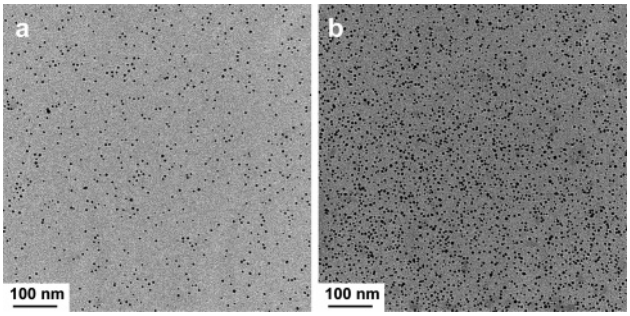

Figure 3. TEM micrographs of HS-PEO(2K) single crystals after incubation with 5 nm AuNPs for (a) 20 and (b) 60 min.

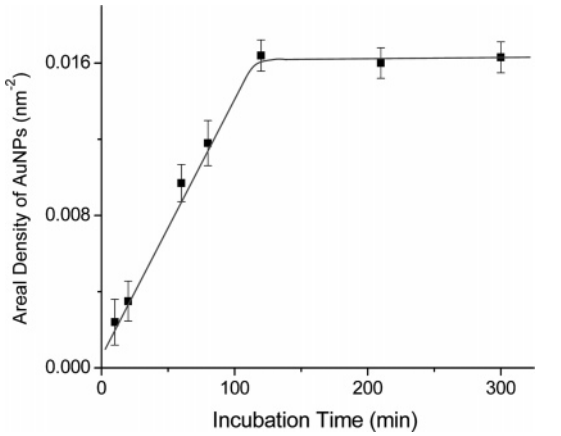

Figure 4. Plot of the areal density of 5 nm AuNPs on HS-PEO(2K) single crystals and the incubation time.

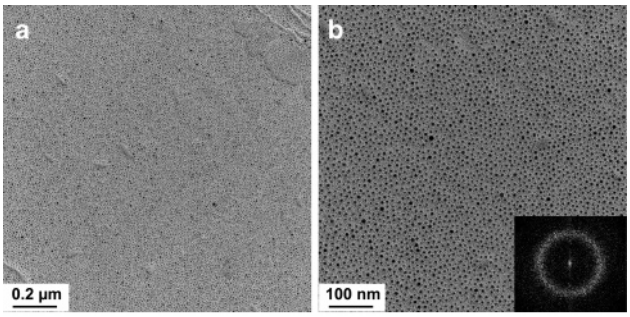

Figure 5. TEM micrographs of the 5 nm AuNP-covered HS-PEO (2K) single crystals after recrystallization. The inset shows the FFT pattern.

was then immersed in the pre-prepared AuNP/amyl acetate colloid for 2 h. After incubation, amyl acetate was used to wash out the free AuNPs.

c. Preparation of Bilayer AuNP/PEO Hybrids. A bilayer AuNP/PEO hybrid consists of two layers of AuNPs and one layer of PEO. It is similar to the structure of multilayer quantum dots on glass substrate.[55] AuNP-covered HS-PEO(2K) single crystals obtained from the previous step were incubated with 1.0% hexanedithiol/amyl acetate solution for 2 h. The samples were washed with amyl acetate before being immersed in gold sol (20 nm) for 2 h. Ethanol was used to wash out the free AuNPs after incubation.

d. Synthesis of Free Binary AuNP Complexes via Bilayer AuNP/PEO Hybrids. The bilayer AuNP/PEO hybrids formed on the glass substrate were placed in ethanol. Ultrasonication was used to bring the hybrids off the glass. PEO single crystals dissolved in ethanol, breaking AuNP layers down to small AuNP complexes. After sonicating for half an hour, one drop of the sample was placed on a carbon-coated Ni grid for transmission electron microscope (TEM) observation.

e. Immobilization of 20 and 50 nm AuNPs on HS-PEO Single Crystals. 10 mL of hexane and 10 mg of sodium oleate were added

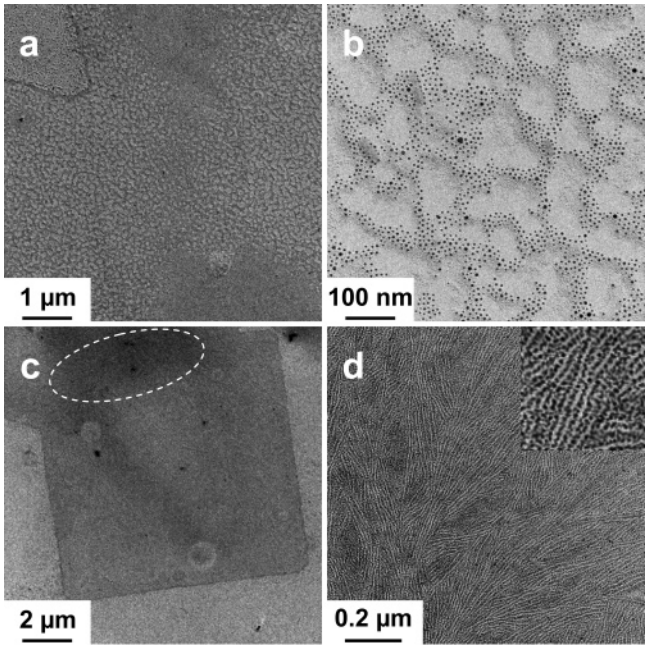

Figure 6. TEM micrographs of the 5 nm AuNP-covered HS-PEO-(2K) single crystals after recrystallization: (a, b) holes; (c, d) fibers. The inset in (d) shows an enlarged area. The samples were shadowed with Pt/Pd.

to 10 g of gold colloid. The mixture was emulsified by vigorous stirring at room temperature for 2 h. 0.12 g of magnesium chloride in 1.5 mL of water was then added with stirring. The mixture was transformed from an emulsion into two liquid phases after 4 h sedimentation. The hexane phase containing AuNPs was collected. A molecular sieve was used to remove the residual water. The HS-PEO(2K) single-crystal suspension was drop-cast on a carbon-coated Ni grid or a piece of glass slide, which was then immersed in the AuNP/hexane colloid for 1 h. Hexane was used to wash out the free AuNPs after incubation.

f. Synthesis of Free Binary AuNP Complexes via Asymmetrically Functionalized 20 nm AuNP Precursors. The 20 nm AuNP-covered HS-PEO(2K) single crystals on the glass substrate were incubated with 1.0% hexanedithiol/amyl acetate solution for 30 min. The sample was washed by amyl acetate thoroughly before being placed in 2.0 g of water. After sonicating for 0.5 h, free asymmetrically functionalized 20 nm AuNPs, which had PEO on one side and hexanedithiol on the other, were dispersed in water. 1.0 g of 5 nm gold sol was then mixed with the obtained asymmetrically functionalized 20 nm AuNPs. The mixture was allowed to react overnight. One drop of the product was placed on a carbon-coated Ni grid for TEM observation. 1 mL of product was transferred to a cuvette for ultraviolet−visible (UV−vis) measurement.

g. Recrystallization of AuNP-Covered HS-PEO Single Crystals. The 5 nm AuNP-covered HS-PEO(2K) single crystals were drop-cast on carbon-coated Ni grids and placed on a hot plate under N_2. The samples were melted at 80 °C for 10 min and then quenched at 50 °C for 24 h.

Characterization. TEM experiments were conducted on a JEOL 2000FX TEM with an accelerating voltage of 120 kV. To enhance contrast, occasionally Pt/Pd was used to shadow the sample before the TEM observation. UV−vis spectra were collected on an Ocean Optics USB4000 miniature fiber-optic spectrometer. The areal density of AuNPs on HS-PEO single crystals was calculated on the basis of TEM images using ImageJ software.

Results and Discussion

Immobilizing AuNPs on HS-PEO Single Crystals. As long chain polymers crystallize from solution or melt, they fold back and forth, forming 2-D lamellae with a typical thickness of 5−10

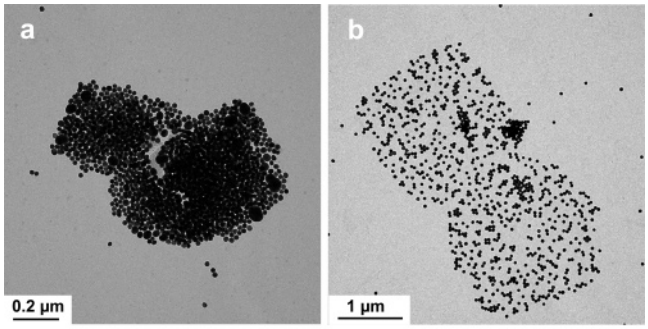

Figure 7. TEM micrographs of HS-PEO(2K) single crystals covered by (a) 20 and (b) 50 nm AuNPs.

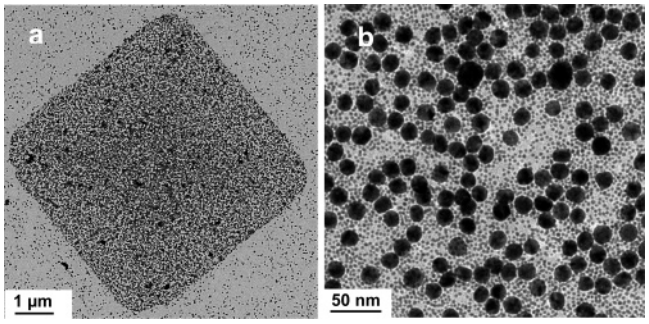

Figure 8. TEM micrographs of the bilayer AuNPs on the surface of HS-PEO(2K) single crystals.

nm. We postulate that if the polymer chains are end-capped with a functional group which can couple with NPs, the NPs should be immobilized on the single-crystal surface, since they do not fit in the lattice. In our preliminary work, HS-PEO was used as the model polymer to study NP immobilization on polymer single crystals. This is because AuNPs can be functionalized with HS-PEO using the "graft-to" method.[56] Furthermore, solution crystallization of PEO has been extensively investigated. Large, uniform single crystals can be easily achieved via solution crystallization.[57] In our study, we used a self-seeding method to obtain uniform PEO single crystals from solution. Figure 1a shows a TEM image of the square-shaped HS-PEO(2K) single crystals obtained by crystallization at 24 °C for 24 h. The sample was shadowed with Pt/Pd, and the thickness of the lamellae can be estimated to be ~12 nm, indicating an extended chain conformation. Hence, for the PEO single crystals shown in the figure, most of the thiol groups are excluded onto the crystal surface upon crystallization. These HS-PEO single crystals were then incubated with TOAB-protected AuNPs (~5 nm in diameter) in amyl acetate for 2 h, and AuNPs were immobilized onto the single-crystal surface because of the formation of Au−S bonds. Figure 1b shows a TEM image of a 6 × 6 μm HS-PEO(2K) single crystal with AuNPs on the surface, and Figure 1c is the enlarged area of Figure 1b. AuNPs can be clearly seen in Figure 1c as the dark dots. Most of the single-crystal surface was covered by the AuNPs. The packing of the particles is rather random, and the average interparticle distance can be estimated to be ~8 nm by using the fast Fourier transform (FFT) of the image. Image analysis also shows that the area per AuNP is ~60 nm^2 and the areal density is ~0.016 nm^{-2}, consistent with the FFT results. A control experiment using a 2K HO-PEO was also conducted. Similar single-crystal structure was formed using solution crystallization. However, after the same incubation procedure, few AuNPs were observed on the HO-PEO single-crystal surface (Figure 1d), which confirms that the formation of the Au−S bonds led to the immobilization of AuNPs on the HS-PEO single-crystal surface.

The areal density of AuNPs is much lower on single crystals with a higher molecular weight as shown in Figure 1e,f. The difference of the AuNP areal densities on 2K and 48.5K HS-PEO single crystals can be attributed to the different thiol group areal densities, as illustrated in Figure 2. For 48.5K PEO, the polymer chain end areal density is much lower than that of 2K PEO (~24 times less, assuming similar lamellar thickness and all thiol groups are on the single-crystal surface). Furthermore, low molecular weight PEO undergoes integral folding which renders most of the chain ends on the crystal surface, while for a relatively long chain PEO, nonintegral folding occurs.[57,58] In this case, despite that thiol groups are different from the rest of the polymer chain, they still can be embedded in the lamellar crystals, as shown in Figure 2a. This further reduces the thiol population on the 48.5K PEO crystal surface. From Figure 1f, we can frequently observe large empty regions on the single-crystal surface which is possibly due to the lack of the surface thiol groups. Therefore, PEO molecular weight can be used as a controlling factor to tune the thiol group (and thus AuNP) areal density on the single-crystal surface.

One challenging task for grafting NPs with polymer chains is to quantitatively control the number of functional groups (chains) on the NP surface. Because of the unique geometry of the PEO single crystals and the AuNPs, the present case allows us to semiquantitatively estimate the number of chains on a single AuNP, detailed as follows. Small AuNPs usually possess cuboctahedral or icosahedral structures.[59−61] For a AuNP with 5 nm diameter, the area of a facet ranges from 2.7 to 6.3 nm^2. Based on the four-chain monoclinic unit cell of PEO with a = 0.796 nm, b = 1.311 nm, c = 1.939 nm, and β = 124.5°, the projection of each unit cell along c-axis (vertical to the lamellar surface) is equal to $ab \sin \beta$ = 0.86 nm^2.[62] Assuming that only one facet of a AuNP can be attached to a PEO single crystal, because the present 2K PEO single crystals possess the extended chain conformation, the probability of finding one thiol group per lattice site is 0.5 on one lamellar surface. Therefore, from the steric hindrance point of view, the maximum number (n^{max}) of the polymer chains which can be coupled onto a AuNP surface ranges from 6 to 14. This indicates that, depending on the crystal facet of a AuNP that is in contact with the PEO single crystal, the average number of the polymer chains attached to the NP is ~10. This number dramatically decreases as the PEO molecular weight increases to 48.5K, in which case it is smaller than 1. n^{max} smaller than 1 indicates that the average area per thiol group is larger than the AuNP facet. Therefore, for 48.5K PEO, the average number of polymer chains attached to a AuNP should be 1, indicating that single-chain functionalized AuNPs were likely achieved.

In addition to PEO molecular weight, the incubation time can also be used to control the areal density of AuNPs. Figure 3 shows the TEM images of 2K HS-PEO single crystal after incubation with AuNPs for 20 and 60 min. Figure 4 is the plot of the areal density of AuNPs vs the incubation time. It is evident that the coupling reaction can be divided into two stages. The first stage is from 0 to ~120 min where the areal density of AuNPs increased linearly with the incubation time. The rate of reaction, in terms of the areal density, is a constant ~1.34 × 10^{-4} nm^{-2} min^{-1}. At ~120 min, the areal density reached to ~0.0164 nm^{-2}, and it remained constant thereafter. Therefore, t > 120 min can be considered as the second stage of the reaction, where the HS-PEO single-crystal surface is saturated with AuNPs.

Recrystallizing AuNP-covered HS-PEO Single Crystals. The order of AuNP packing in the as-prepared samples is

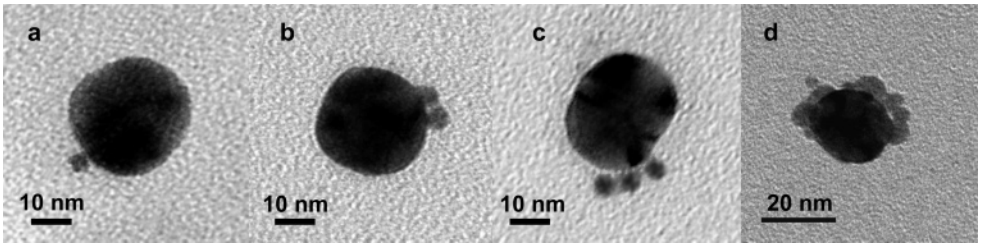

Figure 9. TEM micrographs of the binary AuNP complexes.

Scheme 2. Experimental Procedure To Synthesize Binary AuNP Complexes

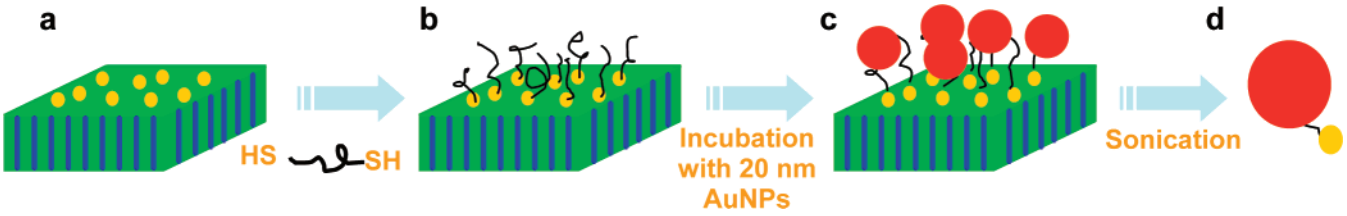

relatively poor, and the interparticle distances vary from 5 to 12 nm. This can be dramatically improved by recrystallization of PEO. Figure 5a,b shows the TEM images of AuNP-covered PEO single crystals after recrystallization. The melting point of 2K HS-PEO is 55 °C. The sample was first melted at 80 °C for 10 min and then recrystallized at 50 °C for 24 h. The shape of the PEO single crystals remained almost unchanged (Figure 6c), and the AuNPs were evenly distributed within the PEO region. For PEO single crystals alone, the square shape cannot be retained under the same experimental procedure because upon melting at 80 °C for 10 min, PEO chains diffuse away from the original single-crystal area. It is thus reasonable to conclude that the AuNPs in the present case retained the crystal morphology of PEO. The possible mechanism is that the AuNPs served as "nanoanchors" for the coupled PEO chains and slowed down their surface diffusion, which in turn helped retain the overall crystal morphology.

In addition to Figure 5, two other distinct morphologies were also observed after recrystallization, as shown in Figure 6. In Figure 6a, numerous holes were seen in the original PEO single-crystal area. Figure 6b shows an enlarged area of Figure 6a. It is evident that the holes were formed due to PEO dewetting on the carbon film. During the dewetting process, the AuNPs migrated with the coupled PEO chains, forming the continuous phase.

Figure 6c,d represents fibrillar morphology observed under the same thermal treatment. Figure 6c shows some fine morphology in the overlapped region of two PEO single crystals (white circle). The enlarged image (Figure 6d) shows the fibrillar structure consisting of AuNP chains. These chains extended along different directions, mimicking a dendrite growth. The average spacing between adjacent AuNP chains is constant ~5.6 nm, which is close to the thickness (6 nm) of the once-folded HS-PEO(2K) lamellae. This indicates that edge-on lamellar crystals of HS-PEO were formed during recrystallization. The thiol groups thus were concentrated between adjacent edge-on lamellar crystals, leading to the formation of AuNP chains. Observing edge-on lamellae in ultrathin film of PEO is of interest in itself. Previous reports suggest that, when the film thickness is smaller than 300 nm, flat-on lamellae dominate while thicker films lead to the coexistence of edge-on and flat-on lamellae.[63,64] In our case, the AuNPs apparently played an important role in the formation process of PEO edge-on lamellae. Detailed investigation is underway to systematically study the formation of AuNP chains using the recrystallization method.

From AFNPs to AuNP Complex. Using the simple incubation method, AuNPs with different sizes can be immobilized on PEO crystals. Figure 7a,b shows the 20 and 50 nm AuNPs immobilized on 2K HS-PEO single crystals. Because of the high contrast of the large size AuNPs, PEO single crystals are not clearly seen. However, the formation of the square-shaped AuNP array is apparently led by the PEO single-crystal templating process.

Because of the planar geometry of PEO single crystals, after the coupling reaction as shown in Scheme 1, the bottom part of a AuNP is functionalized with PEO while the top part is covered with TOAB. Asymmetrically functionalized AuNPs were thus achieved. Note that TOAB can be easily replaced with a variety of functional groups, and this provides a generic means to synthesize asymmetrically functionalized NPs. One simple demonstration is to synthesize a NP complex using NPs with different sizes. To this end, we applied hexanedithiol to functionalize the top portion of the 5 nm AuNP-covered 2K HS-PEO single crystals. A second coupling reaction with the large AuNPs (20 nm) was then carried out as shown in Scheme 2. Bilayer AuNPs were formed on the PEO single-crystal surface (Figure 8a,b). It can be clearly seen that the square-shaped PEO single crystals were covered by AuNPs. AuNPs with different sizes were immobilized onto the PEO single-crystal surface forming a bilayer structure. This unique structure can also be considered as a free-standing film which could offer interesting optic properties. Another advantage of using the polymer-single-crystal-mediating method to synthesize AFNPs is that the solid PEO single-crystal substrate can be easily dissolved, which allows us to obtain free AFNPs as well as binary AuNPs. To this end, the bilayer AuNP/PEO hybrids were sonicated in ethanol for half an hour, and we anticipated observing snowman-shaped binary AuNP complexes, as shown in Scheme 2d. Figure 9a−c shows the TEM images of the resulting complexes. Binary complexes made of AuNPs with two different sizes can be clearly seen from Figure 9a. Interestingly, large AuNPs attached to two or three small AuNPs were also observed (Figure 9b,c).

This observation is not surprising since a 20 nm AuNP was accessible to multiple 5 nm AuNPs during the second coupling process; bonding with hexanedithiol thus led to multiparticle complexes as shown in Figure 9a−c. Note that for all these binary AuNP complexes 5 nm AuNPs stay on only a small part

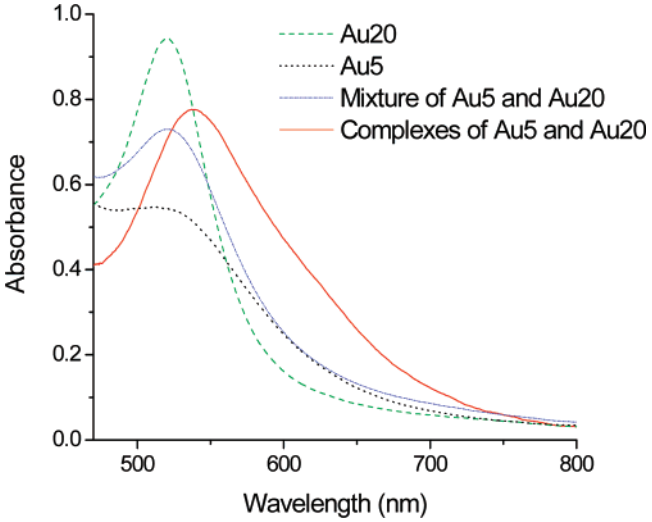

Figure 10. UV−vis spectra of various particles. Au20 and Au5 denote 20 and 5 nm AuNPs, respectively.

of the 20 nm AuNPs, and asymmetric functionalization could thus be confirmed. Similar AuNP complexes were also obtained by mixing free asymmetrically (PEO/hexanedithiol) functionalized 20 nm AuNPs with 5 nm AuNPs in solution, which further confirmed asymmetric functionalization of the AuNPs (Figure 9d). Figure 10 shows the UV−vis spectra of various particles. As 20 nm gold sol was mixed with the 5 nm one, the resultant plasmon resonance was the simple superposition of the individual spectra. However, as the PEO/hexanedithiol functionalized 20 nm AuNPs were mixed with 5 nm gold sol, the final plasmon resonance red-shifted from 520 to 537 nm. It has been reported that coupling AuNPs can induce red shift of the plasmon resonance, so this observation confirmed the formation of AuNP complexes.[65,66]

Conclusions

In summary, we have demonstrated that AuNPs can be immobilized on square-shaped HS-PEO single crystals using an incubation method because of the formation of the Au−S bond. The areal density of AuNPs depends on the polymer molecular weight as well as the incubation time. AuNPs with the size ranging from 5 to 50 nm have been successfully patterned on the HS-PEO single-crystal surface. Because of the planar geometry of the single crystals, only the bottom parts of the AuNPs were attached to the PEO chains, rendering the asymmetric functionalization. By recrystallizing the AuNP-covered HS-PEO single crystals, various morphologies, including AuNP chains, were observed. Free-standing bilayer AuNP/PEO films were obtained by multiple depositions. After subsequent dissolution of the HS-PEO single-crystal substrate, asymmetrical binary AuNP complexes were successfully produced. This approach provides a novel means to pattern AuNPs and to synthesize asymmetrically functionalized AuNPs. We also anticipate that this methodology could be applied to other metal or semiconductor NPs.

Acknowledgment. This work was supported by the NSF CAREER award (DMR-0239415) and CBET-0730738.

References and Notes

(1) Murray, C. B.; Kagan, C. R.; Bawendi, M. G. *Annu. Rev. Mater. Sci.* **2000**, 545−610.
(2) El-Sayed, M. A. *Acc. Chem. Res.* **2001**, *4*, 257−264.
(3) Daniel, M. C.; Astruc, D. *Chem. Rev.* **2004**, *1*, 293−346.
(4) Schmid, G.; Simon, U. *Chem. Commun.* **2005**, *6*, 697−710.
(5) Murphy, C. J.; Gole, A. M.; Hunyadi, S. E.; Orendorff, C. J. *Inorg. Chem.* **2006**, *19*, 7544−7554.
(6) Pileni, M. P. *J. Phys. Chem. B* **2001**, *17*, 3358−3371.
(7) Taleb, A.; Petit, C.; Pileni, M. P. *J. Phys. Chem. B* **1998**, *12*, 2214−2220.
(8) Fendler, J. H. *Chem. Mater.* **2001**, *10*, 3196−3210.
(9) Taleb, A.; Silly, F.; Gusev, A. O.; Charra, F.; Pileni, M. P. *Adv. Mater.* **2000**, *9*, 633−637.
(10) Collier, C. P.; Vossmeyer, T.; Heath, J. R. *Annu. Rev. Phys. Chem.* **1998**, 371−404.
(11) Katz, E.; Willner, I. *Angew. Chem., Int. Ed.* **2004**, *45*, 6042−6108.
(12) Binder, W. H. *Angew. Chem., Int. Ed.* **2005**, *33*, 5172−5175.
(13) Lin, Y.; Skaff, H.; Emrick, T.; Dinsmore, A. D.; Russell, T. P. *Science* **2003**, *5604*, 226−229.
(14) Thompson, R. B.; Ginzburg, V. V.; Matsen, M. W.; Balazs, A. C. *Science* **2001**, *5526*, 2469−2472.
(15) Bockstaller, M. R.; Lapetnikov, Y.; Margel, S.; Thomas, E. L. *J. Am. Chem. Soc.* **2003**, *18*, 5276−5277.
(16) Zhang, Q. L.; Xu, T.; Butterfield, D.; Misner, M. J.; Ryu, D. Y.; Emrick, T.; Russell, T. P. *Nano Lett.* **2005**, *2*, 357−361.
(17) Chiu, J. J.; Kim, B. J.; Kramer, E. J.; Pine, D. J. *J. Am. Chem. Soc.* **2005**, *14*, 5036−5037.
(18) Lopes, W. A.; Jaeger, H. M. *Nature (London)* **2001**, *6865*, 735−738.
(19) Haryono, A.; Binder, W. H. *Small* **2006**, *5*, 600−611.
(20) Zehner, R. W.; Lopes, W. A.; Morkved, T. L.; Jaeger, H.; Sita, L. R. *Langmuir* **1998**, *2*, 241−244.
(21) Sardar, R.; Heap, T. B.; Shumaker-Parry, J. S. *J. Am. Chem. Soc.* **2007**, *17*, 5356−5357.
(22) Deshmukh, R. D.; Buxton, G. A.; Clarke, N.; Composto, R. J. *Macromolecules* **2007**, *17*, 6316−6324.
(23) Darling, S. B.; Yufa, N. A.; Cisse, A. L.; Bader, S. D. *Adv. Mater.* **2005**, *20*, 2446−2450.
(24) Darling, S. B. *J. Vac. Sci. Technol. A* **2007**, 1048−1051.
(25) Zou, S.; Hong, R.; Emrick, T.; Walker, G. C. *Langmuir* **2007**, *4*, 1612−1614.
(26) Balazs, A. C.; Emrick, T.; Russell, T. P. *Science* **2006**, *5802*, 1107−1110.
(27) Darling, S. B. *Surf. Sci.* **2007**, *13*, 2555−2561.
(28) Graeter, S. V.; Huang, J. H.; Perschmann, N.; Lopez-Garcia, M.; Kessler, H.; Ding, J. D.; Spatz, J. P. *Nano Lett.* **2007**, *5*, 1413−1418.
(29) de Gennes, P. G. *Rev. Mod. Phys.* **1992**, *3*, 645−648.
(30) Glotzer, S. C. *Science* **2004**, *5695*, 419−420.
(31) Zhang, Z. L.; Glotzer, S. C. *Nano Lett.* **2004**, *8*, 1407−1413.
(32) de Gennes, P. G. *Croat. Chem. Acta* **1998**, *4*, 833−836.
(33) Gracias, D. H.; Boncheva, M.; Omoregie, O.; Whitesides, G. M. *Appl. Phys. Lett.* **2002**, *15*, 2802−2804.
(34) Manoharan, V. N.; Elsesser, M. T.; Pine, D. J. *Science* **2003**, *5632*, 483−487.
(35) Lu, Y.; Yin, Y. D.; Xia, Y. N. *Adv. Mater.* **2001**, *6*, 415−420.
(36) Shi, W. L.; Zeng, H.; Sahoo, Y.; Ohulchanskyy, T. Y.; Ding, Y.; Wang, Z. L.; Swihart, M.; Prasad, P. N. *Nano Lett.* **2006**, *4*, 875−881.
(37) Snyder, C. E.; Yake, A. M.; Feick, J. D.; Velegol, D. *Langmuir* **2005**, *11*, 4813−4815.
(38) Love, J. C.; Gates, B. D.; Wolfe, D. B.; Paul, K. E.; Whitesides, G. M. *Nano Lett.* **2002**, *8*, 891−894.
(39) Roh, K. H.; Martin, D. C.; Lahann, J. *Nat. Mater.* **2005**, *10*, 759−763.
(40) Roh, K. H.; Martin, D. C.; Lahann, J. *J. Am. Chem. Soc.* **2006**, *21*, 6796−6797.
(41) Mirkin, C. A.; Letsinger, R. L.; Mucic, R. C.; Storhoff, J. J. *Nature (London)* **1996**, *6592*, 607−609.
(42) Alivisatos, A. P.; Johnsson, K. P.; Peng, X. G.; Wilson, T. E.; Loweth, C. J.; Bruchez, M. P.; Schultz, P. G. *Nature (London)* **1996**, *6592*, 609−611.
(43) Mbindyo, J. K. N.; Reiss, B. D.; Martin, B. R.; Keating, C. D.; Natan, M. J.; Mallouk, T. E. *Adv. Mater.* **2001**, *4*, 249−254.
(44) Loweth, C. J.; Caldwell, W. B.; Peng, X. G.; Alivisatos, A. P.; Schultz, P. G. *Angew. Chem., Int. Ed.* **1999**, *12*, 1808−1812.
(45) Zanchet, D.; Micheel, C. M.; Parak, W. J.; Gerion, D.; Williams, S. C.; Alivisatos, A. P. *J. Phys. Chem. B* **2002**, *45*, 11758−11763.
(46) Xu, X. Y.; Rosi, N. L.; Wang, Y. H.; Huo, F. W.; Mirkin, C. A. *J. Am. Chem. Soc.* **2006**, *29*, 9286−9287.
(47) Sung, K. M.; Mosley, D. W.; Peelle, B. R.; Zhang, S. G.; Jacobson, J. M. *J. Am. Chem. Soc.* **2004**, *16*, 5064−5065.
(48) Worden, J. G.; Shaffer, A. W.; Huo, Q. *Chem. Commun.* **2004**, *5*, 518−519.
(49) Liu, X.; Worden, J. G.; Dai, Q.; Zou, J. H.; Wang, J. H.; Huo, Q. *Small* **2006**, *10*, 1126−1129.
(50) Dai, Q.; Worden, J. G.; Trullinger, J.; Huo, Q. *J. Am. Chem. Soc.* **2005**, *22*, 8008−8009.

(51) Shaffer, A. W.; Worden, J. G.; Huo, Q. *Langmuir* **2004**, *19*, 8343−8351.
(52) Jung, G. E. *Combinatorial Peptide and Nonpeptide Libraries: A Handbook*; John Wiley & Sons: New York, 1997.
(53) Fujiki, Y.; Tokunaga, N.; Shinkai, S.; Sada, K. *Angew. Chem., Int. Ed.* **2006**, *29*, 4764−4767.
(54) Li, B.; Li, C. Y. *J. Am. Chem. Soc.* **2007**, *1*, 12−13.
(55) Ouyang, M.; Awschalom, D. D. *Science* **2003**, *5636*, 1074−1078.
(56) Wuelfing, W. P.; Gross, S. M.; Miles, D. T.; Murray, R. W. *J. Am. Chem. Soc.* **1998**, *48*, 12696−12697.
(57) Kovacs, A. J.; Straupe, C.; Gonthier, A. *J. Polym. Sci., Polym. Symp.* **1977**, 31−54.
(58) Cheng, S. Z. D.; Chen, J. H.; Barley, J. S.; Zhang, A. Q.; Habenschuss, A.; Zschack, P. R. *Macromolecules* **1992**, *5*, 1453−1460.
(59) Bovin, J. O.; Malm, J. O. *Z. Phys. D: At., Mol. Clusters* **1991**, *1−4*, 293−298.
(60) C. A.; S. G.; J. U.; K. W. *Z. Phys. D: At., Mol. Clusters* **1991**, *1−4*, 303−306.
(61) Brust, M.; Walker, M.; Bethell, D.; Schiffrin, D. J.; Whyman, R. *J. Chem. Soc., Chem. Commun.* **1994**, *7*, 801−802.
(62) Takahashi, Y.; Tadokoro, H. *Macromolecules* **1973**, 672−675.
(63) Schonherr, H.; Frank, C. W. *Macromolecules* **2003**, *4*, 1188−1198.
(64) Schonherr, H.; Frank, C. W. *Macromolecules* **2003**, *4*, 1199−1208.
(65) Romero, I.; Aizpurua, J.; Bryant, G. W.; de Abajo, F. J. G. *Opt. Express* **2006**, *21*, 9988−9999.
(66) Talley, C. E.; Jackson, J. B.; Oubre, C.; Grady, N. K.; Hollars, C. W.; Lane, S. M.; Huser, T. R.; Nordlander, P.; Halas, N. J. *Nano Lett.* **2005**, *8*, 1569−1574.

MA702047K